Proceedings of the Seventh International Conference on
Railway Technology: Research, Development and Maintenance
Edited by: J. Pombo
Civil-Comp Conferences, Volume 15, Paper 11.13
Civil-Comp Press, Edinburgh, United Kingdom, 2026
ISSN: 2753-3239, doi: 10.4203/ccc.15.11.13

Electromechanical Vibration Control of an HTS Maglev Engineering Prototype Using Electromagnetic Shunt Dampers

W. Zhang[1], M. Yin[1], G. Dovidio[2], Z. Deng[1] and H. Li[1]

[1]Southwest Jiaotong University, Chengdu, China
[2]Interdipartimental Centre of Transport and Sustainable Mobility (CITRraMS), University of L'Aquila, Italy

Abstract

High-temperature superconducting (HTS) maglev systems exhibit inherent advantages such as passive levitation and high stiffness; however, their low intrinsic damping makes them susceptible to vibration under external excitations. In particular, track irregularities and discrete electromagnetic forces from the permanent magnetic guideway (PMG) can induce significant vertical vibration responses, affecting system stability and ride quality. To address this issue, an electromagnetic shunt damper (EMSD) is proposed to enhance the damping performance of HTS maglev systems through electromechanical coupling. An engineering-scale HTS maglev prototype is adopted as the experimental platform. The working principle of EMSD is established, and its effectiveness is validated through on-site experiments. The results show that the root-mean-square (RMS) value of vertical acceleration at the levitation frame is reduced by approximately 30%, demonstrating significant vibration suppression capability. Furthermore, a coupled electromechanical simulation model is developed to investigate system performance under high-speed conditions. Simulation results indicate that EMSD effectively reduces levitation gap fluctuation and improves dynamic performance across a wide range of operating speeds. At 400 km/h, the levitation gap fluctuation is reduced by 24.5%, and similar trends are observed at higher speeds. Overall, the proposed EMSD provides an effective passive and non-contact solution for vibration suppression in HTS maglev systems, with promising potential for engineering applications in high-speed transportation.

Keywords: HTS maglev, electromagnetic shunt damper, electromechanical coupling, vibration suppression, engineering prototype, dynamic performance.

1 Introduction

High-temperature superconducting (HTS) maglev technology has attracted increasing attention as a promising solution for next-generation high-speed transportation systems. Owing to the flux pinning effect in type-II superconductors, HTS maglev systems can achieve passive self-stable levitation without active control[1]. Moreover, the extremely low running resistance makes HTS maglev particularly suitable for high-speed and ultra-high-speed transportation scenarios[2].

Extensive research effortshave been devoted to understanding the electromagnetic characteristics and dynamic behavior of HTS maglev systems[3]. Early studies mainly focused on the interaction between superconducting bulks and permanent magnet guideway (PMG), including levitation and guidance forces[4, 5]. Experimental systems such as SupraTrans in Germany[6] and superconducting maglev prototypes in Brazil[7] have demonstrated the feasibility of this technology. However, most existing studies are limited to laboratory-scale setups, and the dynamic behavior of engineering-scale HTS maglev systems remains insufficiently explored.

A key challenge of HTS maglev systems lies in their extremely low inherent damping[8]. Under track irregularities and discrete magnetic excitation, the vehicle may experience pronounced multi-modal vibration[9]. In particular, the interaction between low-frequency structural modes and higher-frequency electromagnetic excitation leads to complex dynamic responses, which may significantly degrade ride comfort and operational stability.

In China, Southwest Jiaotong University has conducted systematic research on HTS maglev technology for over two decades. As illustrated in Fig 1–Fig 3, the research has evolved from an early laboratory-scale prototype to engineering-scale test systems.
The first stage is the development of the manned HTS maglev test vehicle, as shown in Fig 1[1]. This prototype demonstrated the feasibility of stable levitation and manned operation based on flux pinning. It provided fundamental experimental validation for the HTS maglev concept and laid the foundation for subsequent system development.

Fig 1. The world’s first manned HTS maglev prototype vehicle.

The second stage is the construction of the ring-type HTS maglev experimental line[10], as shown in Fig 2. This platform enabled continuous operation and repeated testing under controlled conditions. It allowed systematic investigation of vehicle dynamics, levitation stability, and operational reliability, marking an important transition from static tests to dynamic experiments.

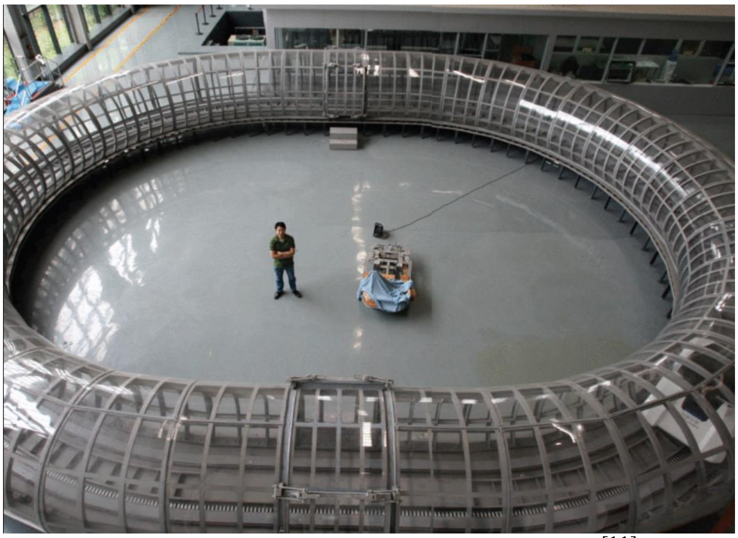

Fig 2. Ring-type HTS maglev test line.[11]

The third stage is the development of the HTS maglev engineering prototype and test line by our team, as shown in Fig 3. This system integrates levitation, guidance, and propulsion subsystems, and is designed to meet practical requirements for large-load and high-speed operation. Compared with previous platforms, it provides a more realistic operating environment and enables comprehensive evaluation of system-level dynamic performance, including vibration characteristics under complex excitation conditions.

Fig 3. High-speed HTS maglev engineering prototype vehicle and test line.

The research presented in this paper is carried out based on this engineering platform, which serves as the foundation for both experimental validation and numerical simulation.

Under actual operation, the HTS maglev system is subjected to various dynamic excitations, including track irregularities and discrete magnetic forces induced by the PMG, as schematically illustrated in Fig 4. PMG irregularities introduce broadband excitation to the system, while the discrete arrangement of the PMG generates periodic electromagnetic forces during vehicle motion. These excitations act on the levitation bogie and are transmitted to the carbody through the suspension system, resulting in coupled vibration responses of the vehicle. Due to the inherent characteristics of HTS levitation, the system exhibits high stiffness but low intrinsic damping, making it more sensitive to external disturbances.

As a result, significant vibration responses may occur, particularly at the levitation-frame level, where the interaction between electromagnetic forces and structural dynamics is most pronounced. These vibration responses not only affect the dynamic performance of the system but also pose potential risks to operational stability and ride comfort.

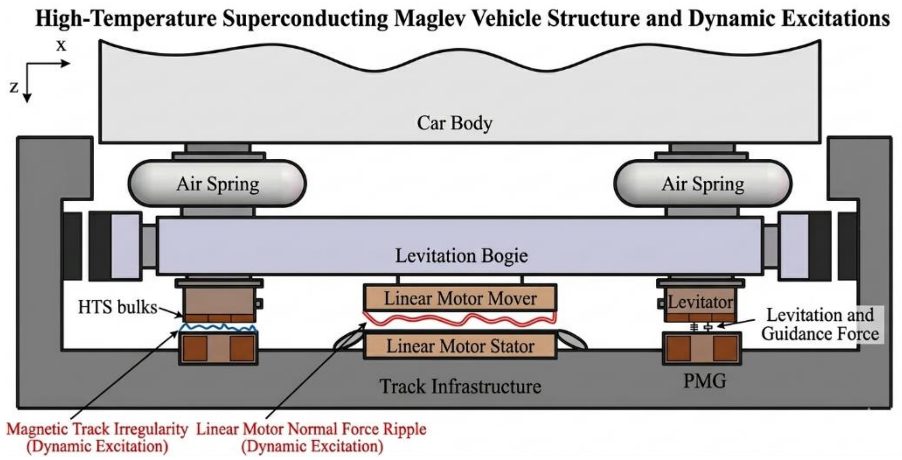

Fig 4. Structure of the HTS maglev vehicle and its dynamic excitation sources, including track irregularities and discrete electromagnetic forces from the PMG.

To improve the damping characteristics of HTS maglev systems, non-contact electromagnetic damping methods have been proposed. Among them, electromagnetic shunt damping (EMSD) introduces additional damping through electromechanical coupling, without affecting the levitation mechanism[12]. This makes EMSD particularly suitable for HTS maglev systems.

Based on the above background, this paper investigates the vibration suppression of an HTS maglev engineering prototype using EMSD. First, the engineering system and vibration characteristics are introduced. Then, the EMSD mechanism is established and implemented on the levitation frame. Comparative experiments are conducted to evaluate vibration responses under different operating conditions. Furthermore, a coupled electromechanical simulation model is developed to analyze system performance under high-speed conditions, with representative results.

2. Electromagnetic Shunt Damping: Principle and Experimental Validation

To enhance the damping performance of the HTS maglev system, an EMSD is introduced based on the principle of electromechanical coupling.

(1) Principle of Electromagnetic Shunt Damping

The working principle of EMSD is illustrated in Fig. 5. When relative motion occurs between the levitation frame and the PMG, the magnetic flux through the coil varies, inducing an electromotive force and current in the circuit. The electrical energy is dissipated through the resistor, converting mechanical vibration energy into electrical energy. At the same time, the induced current generates an electromagnetic force opposite to the motion, providing an equivalent damping effect. As a result, EMSD suppresses vibration through electromechanical coupling without introducing mechanical contact.

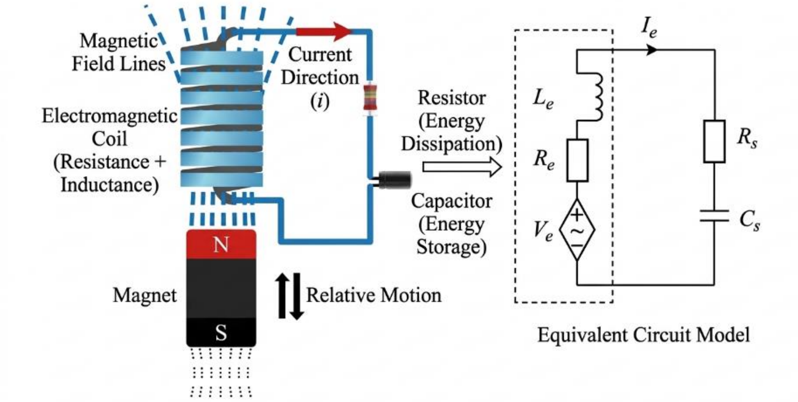

Fig. 5. Working principle and equivalent circuit model of the EMSD

When the levitation frame vibrates relative to the PMG, the magnetic flux through the damping coil varies with time, generating an induced electromotive force (EMF). According to Faraday's law, the induced voltage can be expressed as:

$$v_{ind} = -\frac{d\Phi}{dt} \tag{1}$$

Assuming a linear relationship between the magnetic flux variation and the mechanical motion, the induced voltage is proportional to the vibration velocity:

$$v_{ind} = -k_e \dot{x} \tag{2}$$

where k_e is the electromechanical coupling coefficient and $\dot{x}$ is the generalized velocity.

The EMSD is implemented via a main coil connected to multi-branch RLC shunt circuits. The circuit dynamics can be written as:

$$L\frac{di}{dt}+Ri+\frac{1}{C}\int idt=-k_e\dot{x} \tag{3}$$

The electromagnetic force fed back to the mechanical system is

$$F_{em}=k_e i \tag{4}$$

This force is opposite to the direction of motion and therefore provides an equivalent damping effect. Unlike conventional mechanical damping, EMSD achieves energy dissipation through the electrical circuit, without introducing additional contact or altering the stiffness of the levitation system.

The damping performance of EMSD depends on the circuit parameters. By tuning the electrical parameters to match the dominant vibration frequency, the energy transfer between the mechanical and electrical domains can be maximized, leading to effective vibration suppression.

(2) Experimental Validation on Engineering Prototype

To validate the effectiveness of EMSD, experiments were conducted on the HTS maglev engineering prototype described in Section 2. The installation configuration of the EMSD on the levitation frame and its spatial relationship with the PMG are illustrated in Fig 6.

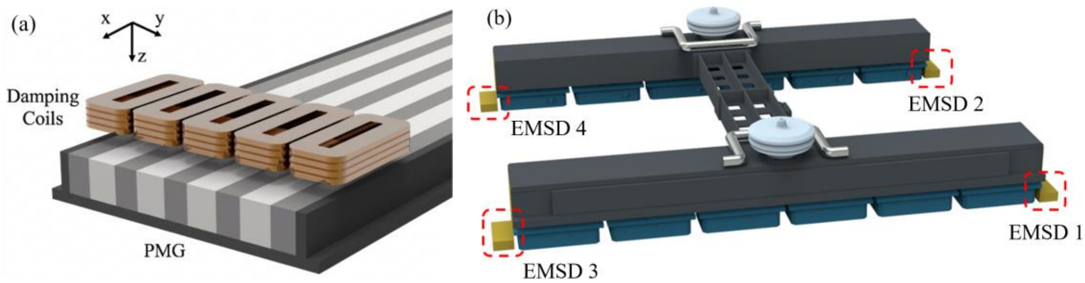

Fig 6. Installation configuration of the electromagnetic shunt damper (EMSD): (a) spatial relationship with the PMG; (b) integration with the levitation frame.

As shown in Fig 6(a), the damping coils are arranged above the PMG in regions with strong magnetic field gradients. The layout is designed according to the magnetic field distribution of the nine-pole Halbach array. Each EMSD unit consists of five coils arranged along the transverse direction of the guideway, corresponding to regions with high vertical magnetic flux density. Adjacent coils are connected in reverse series to maximize the utilization of the magnetic field. Fig 6(b) shows the installation of EMSD on the levitation frame. The damping device, consisting of coil assemblies and mounting fixtures, is rigidly attached to the levitation frame, forming a passive damping unit integrated into the primary suspension system. Multiple EMSD units are symmetrically arranged along the vehicle to ensure balanced damping performance. During operation, the clearance between the EMSD housing and the PMG surface is approximately 8 mm, while the distance between the coil bottom and the PMG surface is about 10 mm. These values ensure effective electromagnetic coupling while maintaining sufficient safety clearance. This configuration enables the

EMSD to operate in regions with strong magnetic field variation, facilitating efficient electromechanical coupling and vibration energy dissipation.

The dynamic responses measured on the levitation frame are presented in Fig 7, including both time-domain and frequency-domain results.

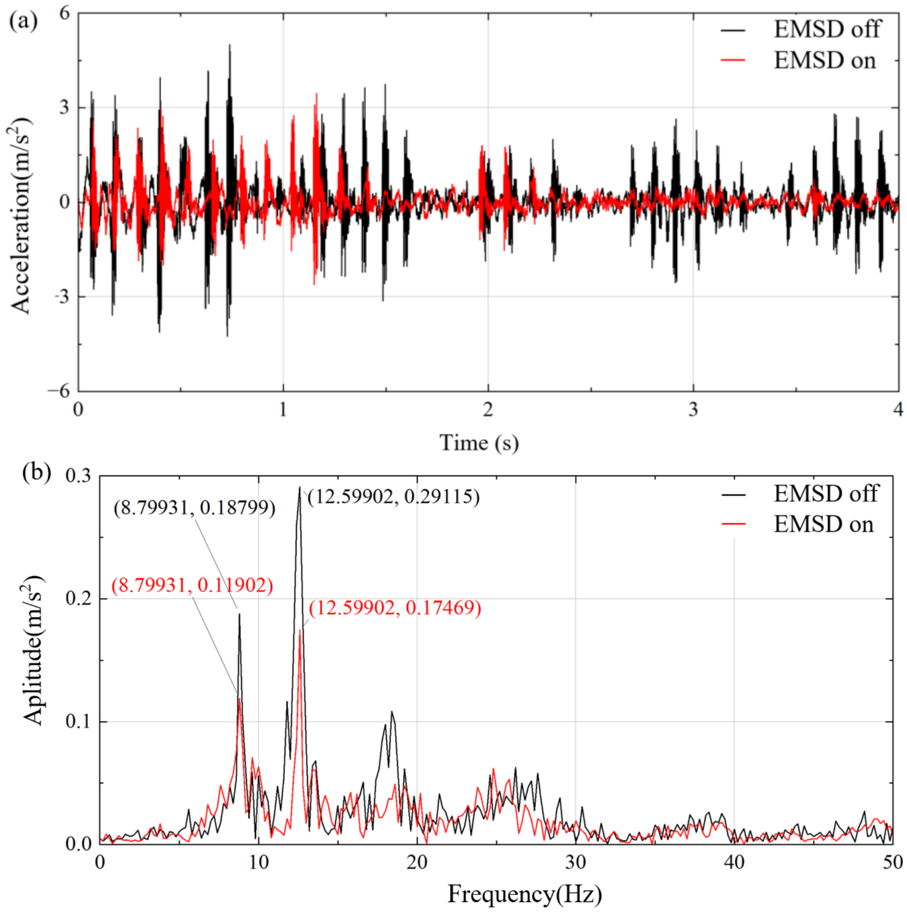

Fig 7. Comparison of vertical acceleration responses of the levitation frame with and without EMSD: (a) time-domain response; (b) frequency-domain spectrum.

As shown in Fig 7(a), when the EMSD is deactivated (open-circuit condition), the vertical acceleration exhibits significant fluctuations, with a maximum peak value of 5.42 m/s² and a root-mean-square (RMS) value of 0.813 m/s². After activating the EMSD (closed-circuit condition), the vibration amplitude is clearly reduced. The peak value decreases to 4.75 m/s², and the RMS value is reduced to 0.575 m/s², corresponding to a reduction of 29.27%. These results indicate that EMSD effectively suppresses the overall vibration intensity. The frequency spectra shown in Fig 7(b) reveal that, under the EMSD-off condition, two dominant peaks appear at approximately 8.8 Hz and 12.6 Hz, with amplitudes of 0.188 m/s² and 0.291 m/s², respectively. When the EMSD is activated, these peak amplitudes are significantly reduced to 0.119 m/s² and 0.175 m/s², corresponding to reductions of 36.7% and 39.9%. The suppression of these dominant frequency components indicates that EMSD effectively attenuates resonance responses. Both the time-domain and frequency-domain results demonstrate that EMSD provides significant vibration suppression for the HTS maglev system. In particular, the reduction of RMS values reflects an overall improvement in vibration level, while the attenuation of spectral peaks confirms the effectiveness of EMSD in suppressing dominant vibration modes.

3 Simulation and Performance Evaluation

To investigate the dynamic performance of the HTS maglev vehicle under high-speed conditions with EMSD, a coupled electromechanical simulation framework is established based on UM and MATLAB/Simulink.

(1) Dynamic Modeling of the HTS Maglev Vehicle System

The vehicle dynamic model consists of one carbody and six levitation frames (bogies), which are connected through the secondary suspension system. As illustrated in Fig 8, the model describes the coupled vibration behavior of the carbody–bogie system under track irregularities.

Fig 8(a) presents the side view of the vehicle model, where the carbody is supported by multiple levitation frames through the suspension system. The primary levitation force is provided by the interaction between the superconducting levitators and the PMG, while the secondary suspension introduces additional stiffness and damping between the carbody and the levitation frames. Fig 8(b) shows the front view of the model, highlighting the vertical and lateral coupling of the system. The carbody and levitation frame are described by multiple degrees of freedom, including vertical displacement, lateral displacement, and rotational motions. The secondary suspension is modeled using equivalent spring-damper elements, while track irregularities are introduced as external excitation inputs acting on the levitation frame.

To incorporate the EMSD into the dynamic simulation, a co-simulation strategy is adopted. The vehicle dynamics are solved in UM, while the EMSD model is implemented in Simulink. During each simulation step, the state variables of the vehicle (such as velocity and displacement of the levitation frame) are transferred to Simulink, where the electromagnetic damping force is calculated. The resulting force is then fed back to the vehicle model, forming a closed-loop electromechanical coupling. To improve computational efficiency, the EMSD model is compiled as a dynamic link library (DLL) and integrated into the UM platform via the external library interface. This approach ensures efficient data exchange and stable numerical performance during simulation. The vehicle dynamic parameters are obtained from Ref.[13], while the EMSD parameters are taken from Ref. [12].

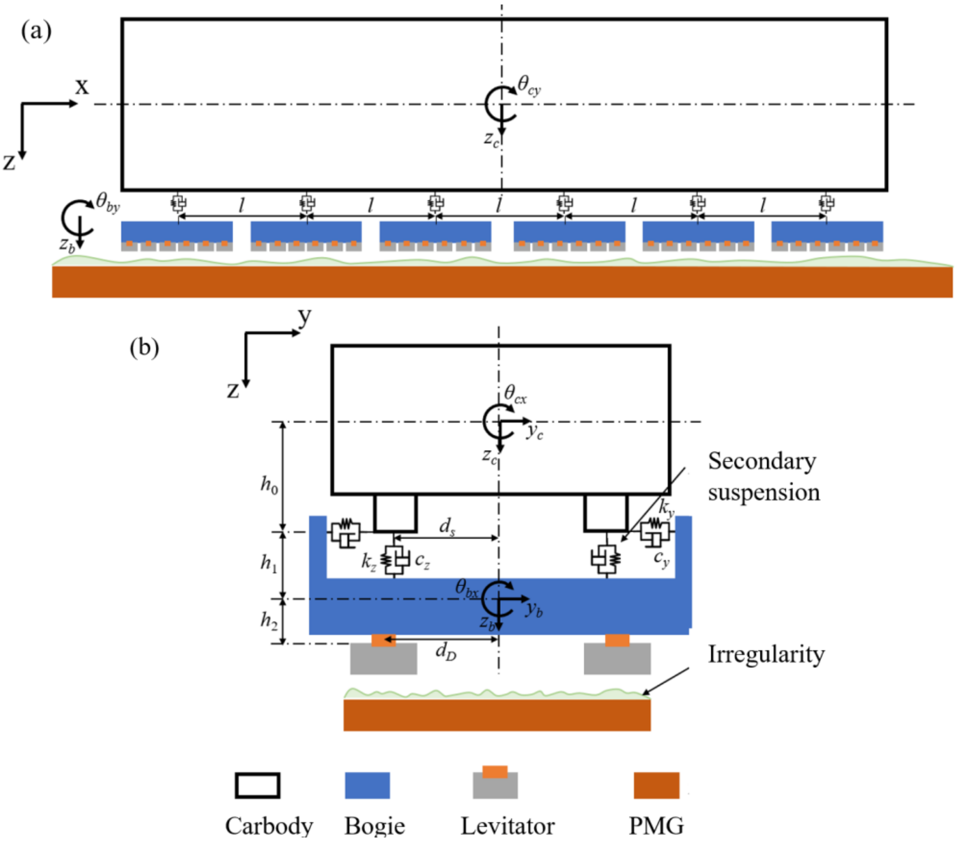

Fig 8. Dynamic model of the HTS maglev vehicle with secondary suspension and track irregularity: (a) side view; (b) front view.

The track irregularity used in the simulation is generated based on a power spectral density (PSD) model to represent realistic guideway excitation. The resulting spatial-domain samples for the left and right PMGs are shown in Fig 9. As illustrated in Fig. 9, the irregularity profiles exhibit random fluctuations along the longitudinal direction, with amplitudes mainly distributed within ±3 mm. The left and right PMGs are generated independently to account for asymmetric excitation, which is essential for capturing the coupled lateral and vertical dynamic responses of the vehicle.

The irregularity signals are constructed by superimposing multiple harmonic components with random phases, ensuring that the generated samples follow the prescribed PSD characteristics. This approach allows the simulation to reproduce realistic broadband excitation conditions encountered in practical operation.

These irregularity inputs are applied to the levitation frames as external excitation, serving as the primary source of vibration in the dynamic simulation. The use of spatial-domain irregularity ensures consistency with vehicle speed when converting to time-domain excitation during simulation.

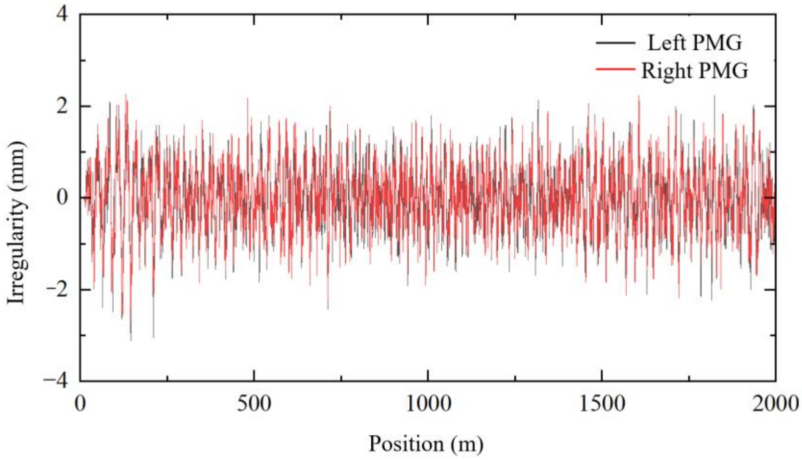

Fig 9. Spatial-domain track irregularity samples for the left and right PMGs generated based on the PSD model

(2) High-Speed Dynamic Response Analysis

The dynamic response of the levitation gap for a representative bogie at a vehicle speed of 400 km/h is shown in Fig. 10. The fluctuation of the levitation gap is a key indicator for evaluating the operational stability of the HTS maglev system. Larger fluctuation amplitudes and smaller minimum gaps increase the risk of mechanical contact between the superconducting levitator and the PMG. As shown in Fig 10, when the EMSD is deactivated, the levitation gap exhibits significant fluctuations. After activating EMSD, the fluctuation amplitude is clearly reduced. Specifically, the peak-to-peak variation decreases from 3.88 mm to 2.93 mm, corresponding to a reduction of 24.5%. In addition, the minimum levitation gap increases from 7.74 mm to 8.98 mm, indicating an improved safety margin during operation.

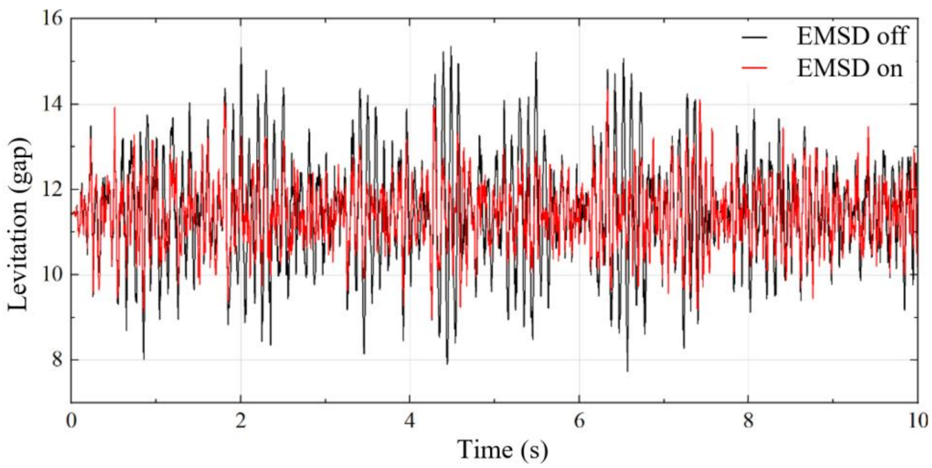

Fig 10. Time-domain response of the levitation gap of the bogie at a speed of 400 km/h under EMSD-off and EMSD-on conditions.

These results demonstrate that EMSD effectively suppresses the fluctuation of the levitation gap and enhances the operational stability of the HTS maglev system, especially under high-speed conditions. This indicates that EMSD improves both vibration performance and operational safety of the system.

The dynamic response of the carbody at a vehicle speed of 400 km/h is shown in Fig 11. Fig 11 compares the vertical acceleration of the carbody under EMSD-off and EMSD-on conditions. It can be observed that the overall vibration level is reduced after applying EMSD. In the time domain, the peak value of vertical acceleration decreases from 0.40 m/s² to 0.36 m/s², corresponding to a reduction of approximately 10%. Compared with the results at the levitation-frame level, the reduction in carbody vibration is less pronounced. This is mainly due to the attenuation effect of the secondary suspension, which weakens the transmission of vibration from the levitation frame to the carbody.

Nevertheless, the reduction in peak acceleration indicates that EMSD still contributes to improving the overall dynamic performance of the vehicle. This demonstrates that the damping effect introduced at the primary suspension level can be effectively transmitted to the carbody, resulting in a global improvement in vibration performance.

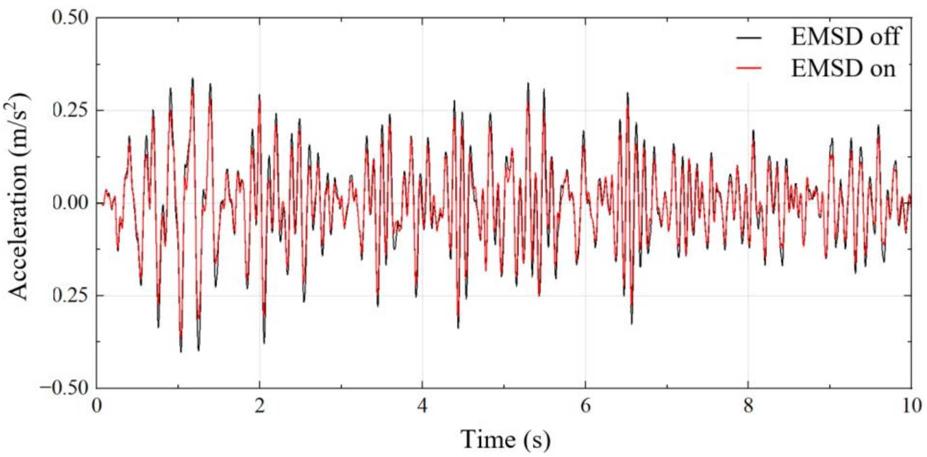

Fig 11. Time-domain response of the vertical acceleration of the carbody at a speed of 400 km/h under EMSD-off and EMSD-on conditions.

To provide a comprehensive evaluation of the dynamic performance under different operating conditions, simulations were carried out at vehicle speeds of 400, 500, and 600 km/h. The results are summarized in Table 1. It can be observed that the introduction of EMSD significantly improves the vibration performance of the levitation frame across all operating conditions. In particular, the vertical acceleration and levitation gap fluctuation are effectively reduced. For example, at a speed of 400 km/h, the RMS value of vertical acceleration of the levitation frame decreases from 2.51 m/s² to 1.92 m/s², corresponding to a reduction of 23.5%. Meanwhile, the peak-to-peak fluctuation of the levitation gap is reduced from 3.88 mm to 2.93 mm, with a reduction of 24.5%.

Similar trends can also be observed at higher speeds. As the vehicle speed increases from 400 km/h to 600 km/h, the vibration level of the system becomes more pronounced, but EMSD continues to provide effective suppression of the levitation-frame response. The reduction in maximum acceleration and RMS values demonstrates that EMSD enhances the equivalent damping of the system under high-speed conditions. However, the improvement in carbody vibration is relatively limited compared with that of the levitation frame. For instance, at 600 km/h, the Sperling index of the carbody is reduced from 1.97 to 1.86, corresponding to a reduction of 5.6%. This indicates that the damping effect introduced at the primary suspension level is partially attenuated by the secondary suspension before being transmitted to the carbody.

Overall, the results demonstrate that EMSD provides effective vibration suppression for the HTS maglev system, particularly at the levitation-frame level, and contributes to improving the overall dynamic performance of the vehicle under high-speed conditions.

Speed (km/h)	400		500		600	
Conditions	EMSD off	EMSD on	EMSD off	EMSD on	EMSD off	EMSD on
Levitation gap fluctuation (mm)	3.88	2.93	3.98	3.16	3.42	3.37
Minimum levitation gap (mm)	7.74	8.98	7.49	8.85	7.18	8.53
Maximum vertical acceleration of levitation bogie (m/s^2)	8.24	6.11	9.46	7.36	10.71	8.24
RMS vertical acceleration of levitation frame (m/s^2)	2.51	1.92	2.88	2.21	3.19	2.44
Maximum vertical acceleration of carbody (m/s^2)	0.4	0.36	0.56	0.46	0.66	0.56
Maximum pitch angular acceleration (rad/s^2)	0.14	0.12	0.21	0.17	0.27	0.22
Vertical Sperling index of the carbody	1.72	1.61	1.84	1.73	1.97	1.86

Table 1. Dynamic performance of the HTS maglev vehicle at different operating speeds

4 Conclusion

This paper investigated the vibration suppression performance of an HTS maglev engineering prototype using an electromagnetic shunt damper (EMSD) based on electromechanical coupling.

First, the working principle of EMSD was established, and its integration with the HTS maglev system was realized through a non-contact damping configuration. Experimental validation on the engineering prototype demonstrated that EMSD effectively reduces the vibration response of the levitation frame. In particular, the root-mean-square (RMS) value of vertical acceleration was reduced by approximately 30%, confirming the effectiveness of EMSD in enhancing system damping.

Furthermore, simulation results under high-speed conditions showed that EMSD maintains its effectiveness across different operating speeds. At 400 km/h, the levitation gap fluctuation was reduced by 24.5%, and the RMS value of vertical acceleration decreased by 23.5%. The improvement remains evident at higher speeds, indicating that EMSD provides stable and robust vibration suppression performance. At the vehicle level, the reduction in carbody vibration is relatively moderate due to the attenuation effect of the secondary suspension. For example, the peak vertical acceleration of the carbody decreases by approximately 10%, and the Sperling index shows a limited but consistent improvement. This indicates that the damping effect introduced at the levitation-frame level can be partially transmitted to the carbody, contributing to overall ride quality enhancement.

Overall, the results demonstrate that EMSD provides an effective passive and non-contact solution for vibration suppression in HTS maglev systems. The proposed approach significantly improves the dynamic performance of the system, particularly at the levitation-frame level, and shows promising potential for application in high-speed HTS maglev transportation.

Acknowledgements

This work was supported in part by the National Natural Science Foundation of China under Grant U24B20125 and Grant 52305133, and in part by the Fundamental Research Funds for the Central Universities under Grant 2682025CX053

References

[1] J. Wang, S. Wang, Y. Zeng, et al., "The first man-loading high temperature superconducting Maglev test vehicle in the world", Physica C, 378, 809-814, 2002.

[2] G. D'Ovidio, F. Crisi, G. Lanzara, "On the magnetic resistance of YBaCuO bulk superconductor dynamically interacting with perturbed flux of iron-homopolar magnetic track", Journal of Optoelectronics and Advanced Materials, 10(5): 1011-1016, 2008.

[3] G. Lanzara, G. D'Ovidio, "Characterization Method of the V-shaped High-Temperature Superconducting Maglev Module for Transport System Application", Journal of Superconductivity and Novel Magnetism, 35(5): 1071-1078, 2022.

[4] L. Kou, Z. Deng, H. Li, et al., "A Two-Dimension Force Model Between High-Temperature Superconducting Bulk YBaCuO and Halbach-Type Permanent Magnet Guideway", IEEE Transactions on Applied Superconductivity, 31(4), 3602208, 2021.

[5] H. Huang, Z. Deng, H. Li, et al., "Numerical Simulation of Dynamic Electromagnetic Characteristics of Superconducting Electrodynamic Suspension (EDS) Train", IEEE Transactions on Applied Superconductivity, 31(5), 3601105, 2021.

[6] L. Schultz, O. de Haas, P. Verges, et al., "Superconductively Levitated Transport System—The SupraTrans Project", IEEE Transactions on Applied Superconductivity, 15(2): 2301-2305, 2005.

[7] G. G. Sotelo, D. H. Nogueira Dias, R. de Andrade, et al., "Tests on a Superconductor Linear Magnetic Bearing of a Full-Scale MagLev Vehicle", IEEE Transactions on Applied Superconductivity, 21(2): 1464-1468, 2005.
[8] J. H. Li, J. Li, D. F. Zhou, et al., "The Modeling and Analysis for the Self-Excited Vibration of the Maglev Vehicle-Bridge Interaction System", Mathematical problems in engineering, 2015(1), 709583, 2015.
[9] H. Li, S. Wang, S. Liu, et al., "Lateral-vertical coupled nonlinear vibration characteristics of HTS maglev based on multiscale method and experimental test", Mechanical Systems and Signal Processing, 240, 113449, 2025.
[10] Z. Deng, W. Zhang, J. Zheng, et al., "A High-Temperature Superconducting Maglev Ring Test Line Developed in Chengdu, China", IEEE Transactions on Applied Superconductivity, 26(6), 3602408, 2016.
[11] "A super chute [The Big Picture]", IEEE Spectrum, 51(7): 20-21, 2014.
[12] H. Li, Y. He, L. Wang, et al., "Enhancing lateral dynamic performance of HTS Maglev vehicles using electromagnetic shunt dampers: optimisation and experimental validation", Vehicle System Dynamics, 2025: doi.org/10.1080/00423114.2025.2510533.
[13] S. Wang, H. Li, L. Wang, et al., "Suspension Parameters Optimization of HTS Maglev Under Random Vibration". IEEE Transactions on Applied Superconductivity, 31(8), 3603704, 2021.